Electronic Supplementary Information

Single-Crystalline Ordered Mesoporous Indium Tin Oxides with Controlled Sn/In Ratio via Vapor-Phase Oxidation of Metal Chlorides within Silica Colloidal Crystals

Tomohiro Okita,[a] Ryoma Uchida,[a] Atsushi Shimojima,[a,b,c] and Takamichi Matsuno[*a,b,c]

[a] Department of Applied Chemistry, Faculty of Science and Engineering, Waseda University, 3-4-1 Okubo, Shinjuku-ku, Tokyo 169-8555, Japan.

[b] Waseda Research Institute for Science and Engineering, Waseda University, 3-4-1 Okubo, Shinjuku-ku, Tokyo 169-8555, Japan.

[c] Kagami Memorial Research Institute for Materials Science and Technology, Waseda University, 2-8-26 Nishiwaseda, Shinjuku-ku, Tokyo 169-0051, Japan.

E-mail: matsuno@aoni.waseda.jp

Table of Contents

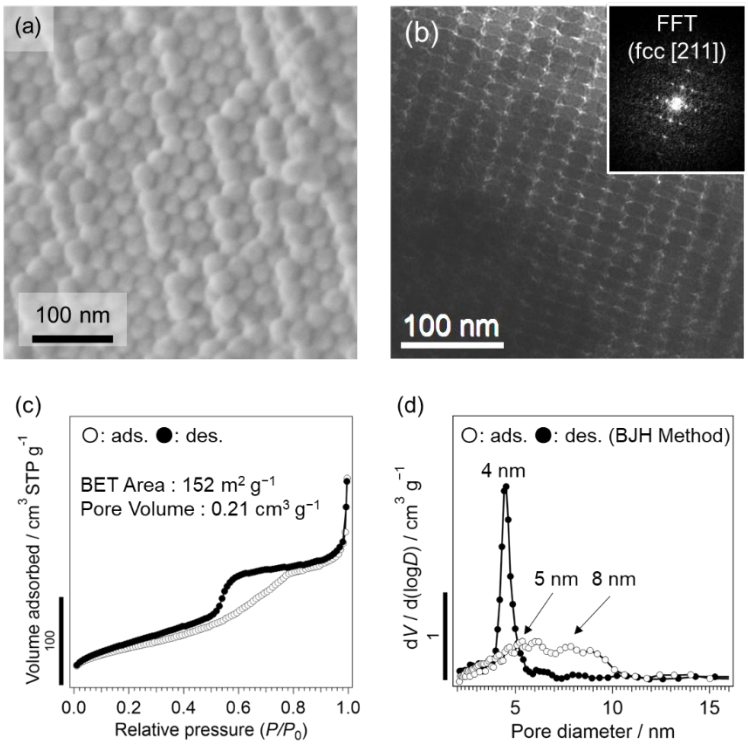

Fig. S1 (a) SEM image, (b) TEM image (inset: FFT pattern), (c) N_2 adsorption–desorption isotherms, and (d) BJH pore diameter distributions of SCCs-29 (○: adsorption, ●: desorption).

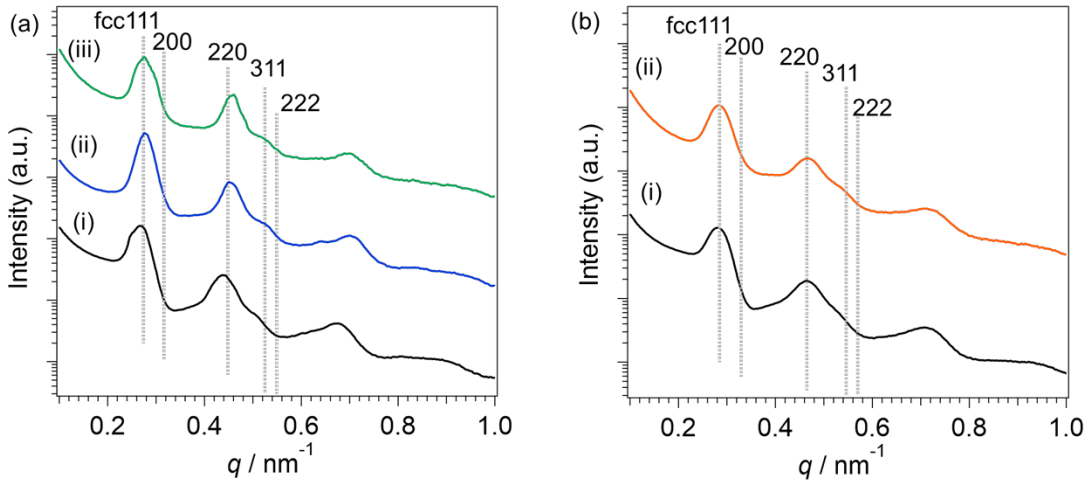

Fig. S2 SAXS patterns of (a-i) SCCs-29, (a-ii) ITO-29, (a-iii) ITO-29-pre, (b-i) SCC-30, and (b-ii) ITO-30-0.2-dil.

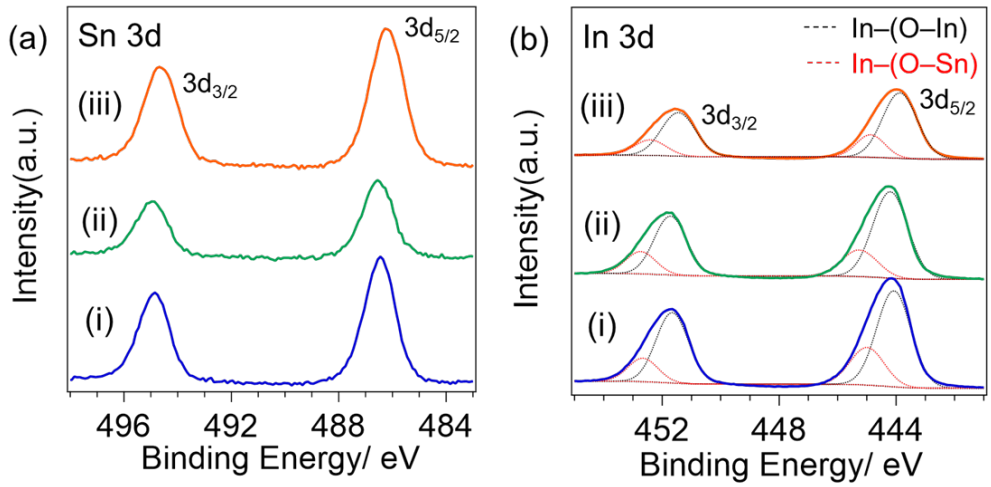

Fig. S3 XPS spectra of (a) Sn 3d, (b) In 3d. (i) ITO-29, (ii) ITO-29-pre, (iii) ITO-30-0.2-dil.

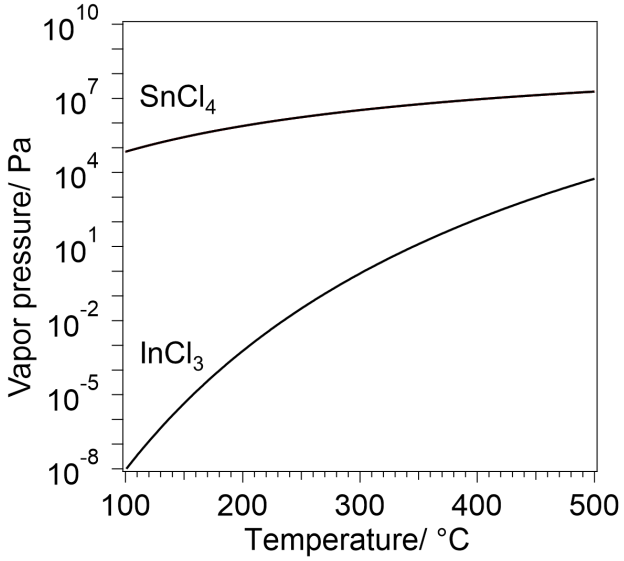

Fig. S4 Vapor pressure–temperature curves of $InCl_3$ and $SnCl_4$. This graph was prepared using data and calculations from refs 1 and 2.

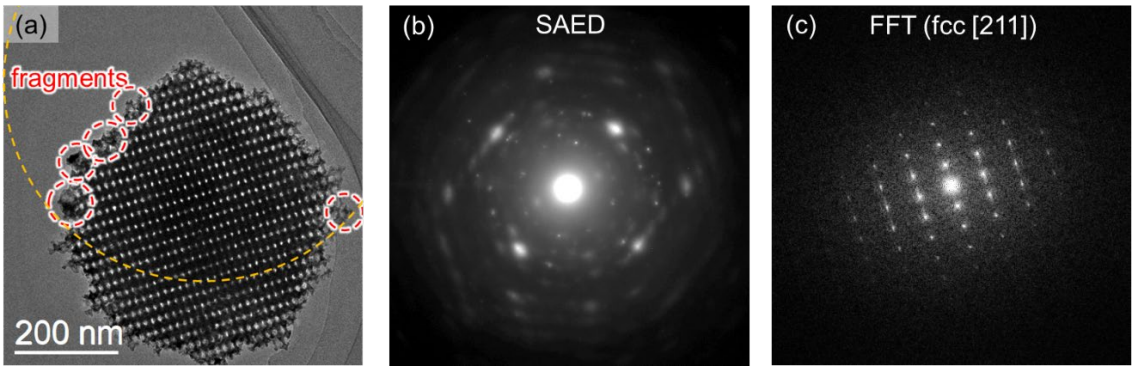

Fig. S5 (a) TEM image, (b) SAED pattern corresponding to the orange circle in (a), and (c) FFT pattern of ITO-29.

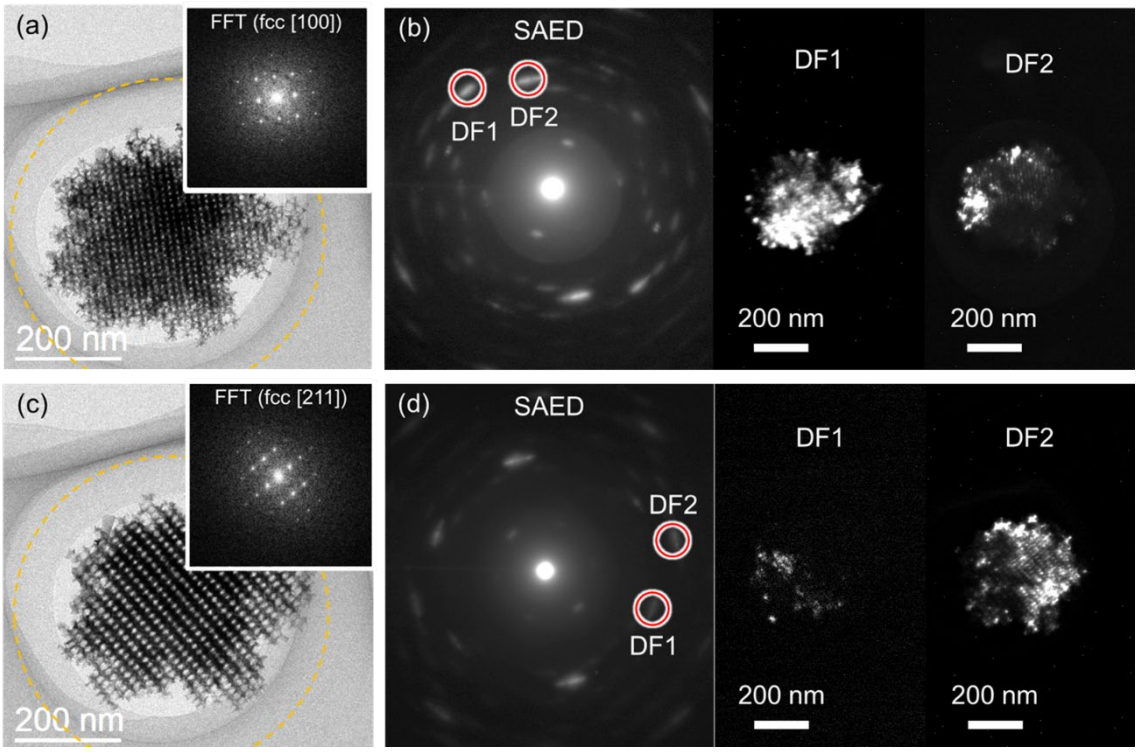

Fig. S6 (a,c) TEM images (inset: FFT pattern), (b,d) corresponding SAED patterns and DF-TEM images of ITO-30-0.2-dil.

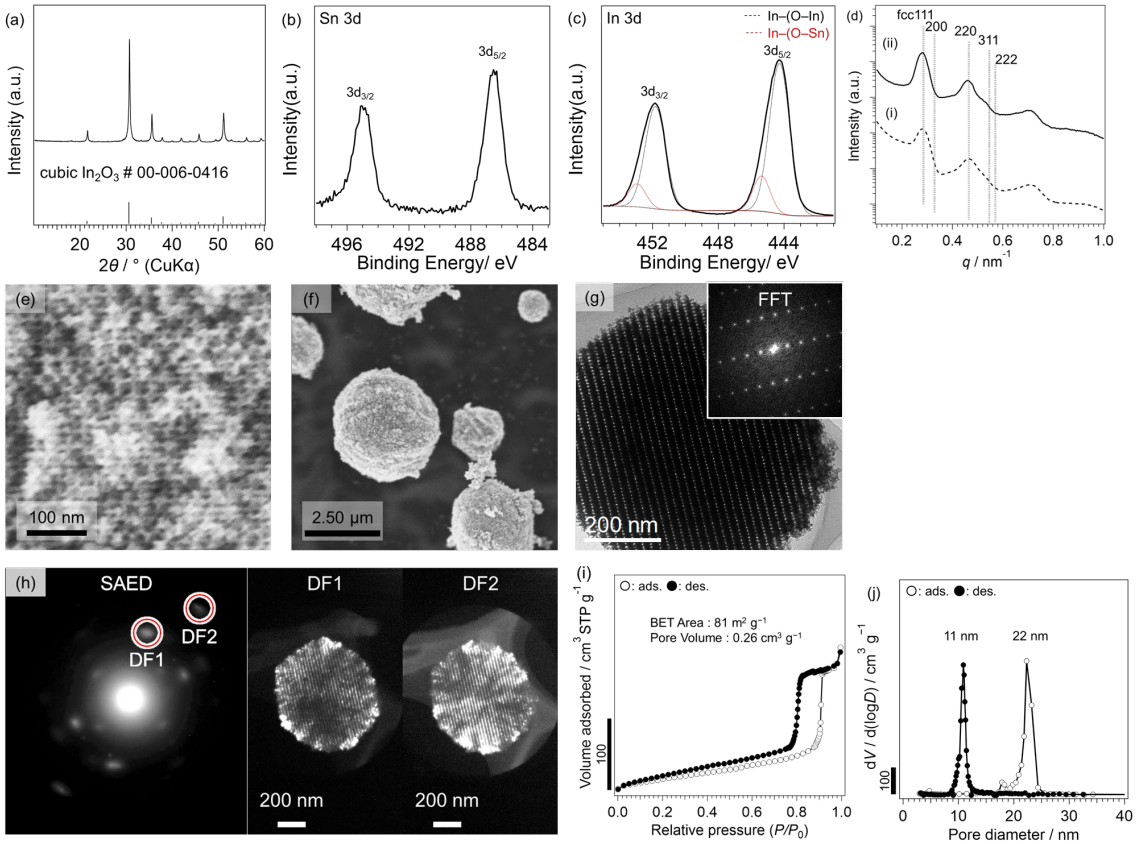

Fig. S7 (a) XRD pattern and (b) and (c) XPS spectra of ITO-30-0.2 ((b) Sn 3d, (c) In 3d). (d) SAXS pattern of (i) SCCs-30 and (ii) ITO-30-0.2. (e) Magnified SEM image, (f) SEM image, (g) TEM image (inset: FFT pattern), and (h) SAED pattern and corresponding DF-TEM images of ITO-30-0.2. (i) N_2 adsorption–desorption isotherms, and (j) BJH pore diameter distributions of ITO-30-0.2 (○: adsorption, ●: desorption).

Geometrical calculation of the pore volume and the specific surface area of mesoporous ITOs.

Geometrical surface area and pore volume were calculated assuming that the mesoporous ITO has an ideal fcc structure (Porosity: 74%).

1. Geometrical calculation for the surface area (S_{ideal})

$$S_{ideal} = \frac{N_{silica} \times S_{silica}}{V_{ITO} \times \rho_{ITO}} = \frac{4 \times 4\pi r^2}{\left(\frac{100-74}{74} \times 4 \times \frac{4}{3}\pi r^3\right) \times 7.16} \times 10^4 \ [\mathrm{m^2\ g^{-1}}]$$
$$= \frac{0.12}{r} \times 10^4 \ [\mathrm{m^2\ g^{-1}}]$$

(N_{silica}: number of silica nanospheres in the unit cell of fcc structure, S_{silica}: geometrical surface area of silica nanospheres in the unit cell of fcc structure, V_{ITO}: volume of ITO in the unit cell of fcc structure, ρ_{ITO}: density of ITO (7.16 g cm^{-3}), r_{silica}: average radius of silica nanospheres [nm])

2. Geometrical calculation for the pore volume (V_{ideal})

$$V_{ideal} = \frac{N_{silica} \times V_{silica}}{V_{ITO} \times \rho_{ITO}} = \frac{4 \times \frac{4}{3}\pi r^3}{\left(\frac{100-74}{74} \times 4 \times \frac{4}{3}\pi r^3\right) \times 7.16} = 0.40 \ [\mathrm{cm^3\ g^{-1}}]$$

(V_{silica}: Volume of silica nanospheres in the unit cell of fcc structure)

Calculation for the volume proportion of mesoporous particles in mesoporous ITOs.

The volume ratio of the mesoporous particles was calculated from the ideal pore volume of mesoporous ITO and the experimentally measured value from N_2 adsorption–desorption measurements. The volumes used in the calculation were illustrated in Fig. S6.

1. Calculation of weight ratio (x_w) of mesoporous particles

$$x_w = \frac{V_{N2}}{V_{ideal}} \times 100\ [\%]$$

(V_{N2}: Pore volume of mesoporous ITO measured by N_2 adsorption–desorption measurements)

2. Calculation of volume ratio (x_v) of mesoporous particles

$$x_v = \frac{V_{wall} + V_{pore}}{V_{wall} + V_{pore} + V_{dense}} \times 100\ [\%]$$

$$= \frac{\left(\frac{x_w}{\rho_{ITO}}\right) + \left(\frac{x_w}{\rho_{ITO}}\right) \times \left(\frac{\frac{\sqrt{2}}{6}\pi}{1 - \frac{\sqrt{2}}{6}\pi}\right)}{\left(\frac{x_w}{\rho_{ITO}}\right) + \left(\frac{x_w}{\rho_{ITO}}\right) \times \left(\frac{\frac{\sqrt{2}}{6}\pi}{1 - \frac{\sqrt{2}}{6}\pi}\right) + \left(\frac{1 - x_w}{\rho_{ITO}}\right)} \times 100\ [\%]$$

(V_{wall}: volume of the pore walls of the mesoporous ITO per unit weight of ITO, V_{pore}: volume of the mesopores in the mesoporous ITO per unit weight of ITO, V_{dense}: volume of the non-porous ITO per unit weight of ITO)

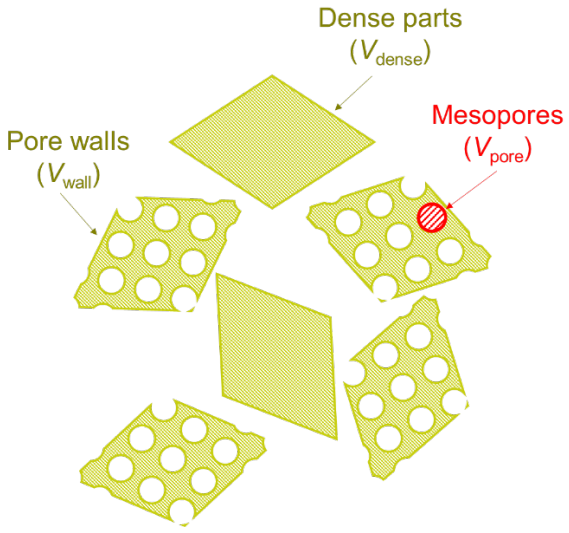

Fig. S8 Schematic image of V_{dense}, V_{wall}, and V_{pore} used in the calculation for the volume proportion of mesoporous ITO.

References

(1) R. Chanson, S. Bouchoule, C. Cardinaud, C. Petit-Etienne, E. Cambril, A. Rhallabi, S. Guilet and E. Blanquet, *J. Vac. Sci. Technol. B*, 2014, **32**, 011219.

(2) D. R. Stull, *Ind. Eng. Chem.*, 1947, **39**, 517.